Available online at www.sciencedirect.com
ScienceDirect
Mendeleev Commun., 2017, **27**, 615–617

Mendeleev
Communications

Diphenylacetylene hydrogenation on a PdAg/Al_2O_3 single-atom catalyst: an experimental and DFT study

**Aleksandr V. Rassolov, Dmitry S. Krivoruchenko, Michael G. Medvedev,
Igor S. Mashkovsky, Aleksandr Yu. Stakheev* and Igor V. Svitanko**

*N. D. Zelinsky Institute of Organic Chemistry, Russian Academy of Sciences, 119991 Moscow,
Russian Federation. Fax: +7 499 135 5328; e-mail: st@ioc.ac.ru*

DOI: 10.1016/j.mencom.2017.11.026

The hydrogenation of diphenylacetylene (DPA) on palladium–silver catalysts with a single-atom structure was investigated. It has been shown experimentally that the reaction rate of alkene to alkane hydrogenation is substantially lower than the rate of DPA semi-hydrogenation. The kinetic barriers of all stages of hydrogenation were calculated by the DFT method.

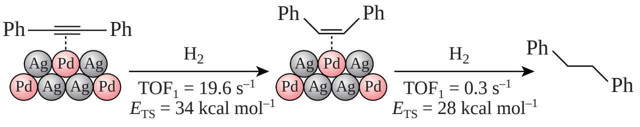

It is well known that the selectivity of metal supported catalysts is dramatically limited by different coordinative unsaturation of metal atoms (corner, edge and plane atoms) on the surface of metal nanoparticles. Therefore, the synthesis of selective and active heterogeneous catalysts with the uniform structures of active sites is a fundamental challenge in heterogeneous catalysis.[1,2]

Recently, attention has been focused on a methodology for the preparation of catalysts with active sites as isolated metal atoms, which are referred to as single-atom catalysts (SACs).[3–5] SACs can be obtained *via* different techniques like co-precipitation, high-vacuum physical deposition (sputtering or atomic-layer deposition) and alloying with a second metal.[3,6–7]

The alloying with the second metal is promising for the SAC structure wherein active metal atoms are isolated by the atoms of an inactive metal.[8,9] The main advantages of SACs are the following: (1) more active component is present in the surface of the host metal at very low concentrations and (2) atoms of the active component are thermodynamically more stable when surrounded by the host metal atoms.[10] This technique also allows one to completely use all SAC benefits providing a great potential to significantly improve catalytic performance for a number of chemical reactions. For example, the possibility of effective elimination of alkyne multi-bonded adsorption makes SAC an ideal for the semi-hydrogenation of acetylenic compounds giving optimum selectivity for alkene formation.

Previously, the detailed characterization of $PdAg_2/\alpha\text{-}Al_2O_3$ supported catalysts revealed the formation of bimetallic PdAg nanoparticles with Pd single atoms on their surface.[11] It was shown by H_2-TPR that the Pd and Ag components were reduced almost simultaneously in a range of 15–200 °C with two maxima at 30 and 65 °C, which corresponded to the reduction of palladium and silver with the formation of PdAg. The relative narrowness of the reduction interval for a $PdAg_2/\alpha\text{-}Al_2O_3$ catalyst in comparison with PdAg samples supported on $\gamma\text{-}Al_2O_3$ and $MgAl_2O_4$ can be attributed to the fact that, on the $\alpha\text{-}Al_2O_3$ surface, the particles of the initial $PdAg_2(OAc)_4(HOAc)_4$ complex are much larger than the similar particles formed on the other supports, as was indicated by TEM.[11] Excellent selectivity towards olefin formation was shown with these catalysts in the hydrogenation of substituted alkynes presumably due to the exception of multipoint adsorption.[12] However, the fundamental question remained open concerning the specific catalytic activity of a single-atom Pd site in PdAg composition compared to the specific catalytic activity of Pd atoms on the surface of monometallic particles.

Here, we report a study of the selective liquid-phase hydrogenation of diphenylacetylene (DPA). This reaction is of great importance because the olefinic products of semi-hydrogenation can be used as parent materials in fine organic chemistry and food, pharmaceutical and electronics industries. The reaction was carried out on a $PdAg_2/Al_2O_3$ catalyst with a single-atom structure, as confirmed by FTIR-CO analysis (see below). The obtained data on $PdAg/Al_2O_3$ specific catalytic activity (turnover frequency, TOF) were compared with data for a monometallic Pd/Al_2O_3 catalyst. Considering that hydrogenation occurs as a two-stage reaction [(1) alkyne-to-alkene and (2) alkene-to-alkane hydrogenation] TOF was evaluated for both of them.[†]

The catalysts were characterized by TEM and FTIR-CO. Dark areas in the TEM microphotographs are responsible for metal particles (Figure 1). It is evident that spherical metal particles with a size of 5–10 nm are evenly distributed over the support structure.

The FTIR spectra of adsorbed CO for Pd/Al_2O_3 and $PdAg_2/Al_2O_3$ are shown in Figure 2. In a range of 2200–1800 cm^{-1}, several peaks associated with CO adsorption on Pd species can be observed. The spectrum of the reference monometallic Pd/Al_2O_3 exhibits two bands assigned to linearly adsorbed CO on atop sites Pd^0 (an asymmetric band at 2088 cm^{-1}) and to bridge-like

---

[†] The Pd–Ag catalysts were prepared by the incipient-wetness impregnation of Al_2O_3 (Sasol, S_{BET} = 56 $m^2\ g^{-1}$) with a solution of the $PdAg_2(OAc)_4(HOAc)_4$ complex[13] in dilute acetic acid (pH 2.8). The sample was air-dried at room temperature and activated in a 5 vol% H_2/Ar flow (550 °C, 2 h) without preliminary calcination. It was demonstrated earlier that these conditions ensure the formation of compositionally identical bimetallic particles.[14] The resulting catalysts contained 1 wt% Pd and 2 wt% Ag. Monometallic Pd/Al_2O_3 sample with 1 wt% Pd was also prepared by incipient-wetness impregnation with an aqueous solution of $Pd(NO_3)_2$. After air drying at room temperature, the sample was calcined at 500 °C (air, 4 h) and reduced at 500 °C (5% H_2/Ar, 1 h). For details of the calculations and characterization, see Online Supplementary Materials.

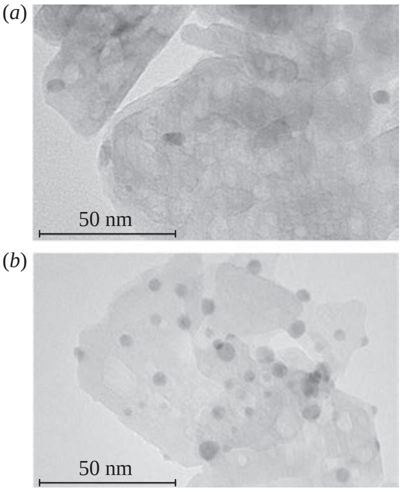

Figure 1 TEM images of (*a*) Pd/Al_2O_3 and (*b*) $PdAg_2/Al_2O_3$ catalysts.

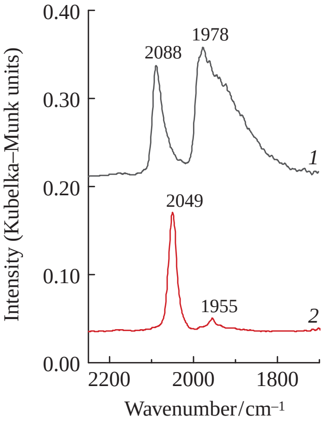

Figure 2 FTIR-CO spectra for (*1*) Pd/Al_2O_3 and (*2*) PdAg/Al_2O_3.

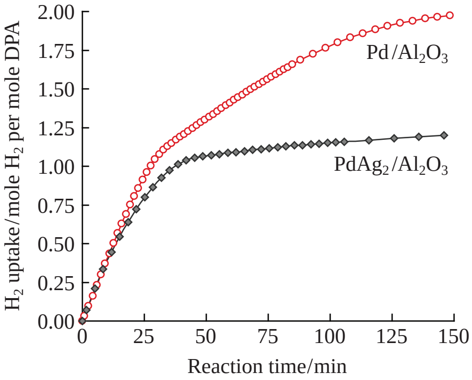

Figure 3 The time dependence of hydrogen uptake for Pd/Al_2O_3 and 1% Pd–2% Ag_2/Al_2O_3 catalysts in the liquid-phase hydrogenation of diphenylacetylene. P_{H_2} = 5 bar, *m* = 1.5 mg.

adsorbed CO (a wide band at 1978 cm^{-1}).[15–17] In the case of the bimetallic system, only one intense band at 2049 cm^{-1} was detected in the spectrum, which can be attributed to CO bonded linearly on metallic palladium. The intensity of a bridge-like CO band at 1955 cm^{-1} is essentially negligible. Thus, FTIR-CO data clearly indicate that Pd atoms on the surface of Pd–Ag bimetallic nanoparticles are predominantly isolated from each other by silver atoms forming a single-atom structure. Previously, a similar surface structure was observed for a PdIn/Al_2O_3 catalyst.[18]

Figure 3 shows the kinetics of H_2 consumption. To minimize errors in the determination of reaction rate, the catalyst amounts were selected in such a way as to provide approximately the same reaction rate at the first stage in accordance with a previously discussed methodology.[11] It is evident that the activities of Pd/Al_2O_3 and $PdAg_2/Al_2O_3$ are similar at a stage of C≡C bond hydrogenation (consumption of 1 equiv. H_2). However, after the consumption of 1 equiv. H_2, the hydrogenation rate on the single-atom $PdAg_2/Al_2O_3$ becomes significantly lower than that on monometallic Pd/Al_2O_3. TOFs calculated based on chemisorption data and 90% selectivity are given in Table 1. Interestingly, the TOF_1 (triple-to-double bond hydrogenation) over PdAg SAC was higher than that over Pd by a factor of about 1.5. The observed increase in TOF_1 may be attributed to the suppression of di-sigma olefin or alkyne adsorption since multiatomic Pd active sites are essentially absent on the surface of PdAg particles.

The TOF_2 calculated for a second reaction stage (complete hydrogenation of target alkene to alkane) was lower by a factor of almost 11 for PdAg in comparison with a Pd catalyst. As a result, the TOF_1/TOF_2 ratio notably increased for $PdAg_2/Al_2O_3$ (from 4 up to 66). This significant inhibition of the undesired double bond hydrogenation favors effective kinetic control of the reaction and selectivity for olefin formation (Table 1). Selectivity increased from ~91 to ~97% for $PdAg_2/Al_2O_3$ in comparison with monometallic Pd/Al_2O_3.

In order to understand the reasons for a significantly slower reaction rate at the second stage of SAC, the reaction pathway was studied in detail by DFT at the PBE0[19]-D3[20]/IMCP-SR1[21,22]//PBE0-D3/SBKJC[23] level of theory (for details, see Online Supplementary Materials). The PBE0 functional was chosen as it is known to be accurate for organic chemistry calculations[24] and has recently been shown to be well-grounded in theory[25] and the IMCP-SR1 basis set was chosen as it incorporates scalar-relativistic effects, which are important for heavy elements such as palladium and silver in our case,[26] and retains the correct nodal structures of atoms.[22] Figure 4 shows the computed energy profile for DPA hydrogenation over PdAg catalyst surfaces with isolated Pd atom sites occurring by a step-by-step hydrogenation mechanism with active H species. The DPA is adsorbed and well activated on the two neighboring Pd sites of Pd–Ag–Pd clusters, and is thermodynamically favored to be hydrogenated to diphenylethylene (DPE) through an ethylene-like C_2Ph_2HPd intermediate by active hydrogen species on the Pd single active sites, with the second elementary step being exothermic. The calculated kinetic barriers of this two-step hydrogenation were 34 (TS1) and 15.5 kcal mol^{-1} (TS2) on the PdAg surface, suggesting that such a PdAg catalyst is sufficiently active in triple carbon–carbon bond hydrogenation.

Note that the appropriate arrangement of Pd single sites on the Pd–Ag–Pd clusters provides two neighboring Pd isolated sites for DPA adsorption with moderate σ-bonding, which results in C≡C bond activation through an ethylene-like intermediate and facile conversion into DPE. The single Pd active sites of PdAg are also efficient for the activation of H_2 to hydrogen active species.

Table 1 Kinetic parameters of liquid-phase alkyne hydrogenation calculated based on CO chemisorption data.

Catalyst	r_1/mol$_{H_2}$ mg$_{cat}^{-1}$ min^{-1}	r_2/mol$_{H_2}$ g$_{cat}^{-1}$ min^{-1}	TOF_1/s^{-1}	TOF_2/s^{-1}	TOF_1/TOF_2	$S_=$ (%)[a]
0.5% Pd/Al_2O_3	13.07	3.36	13.2	3.32	4.0	91.2
1% Pd–2% Ag_2/Al_2O_3	10.27	0.15	19.6	0.30	65.6	96.6

[a] At a 90% DPA conversion.

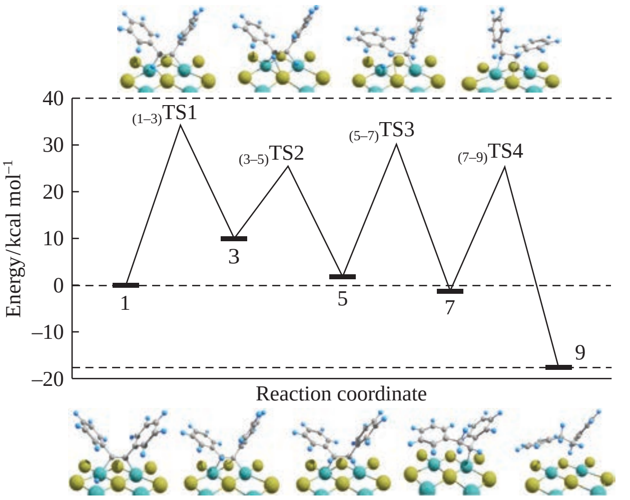

Figure 4 Energy profile for the step-by-step mechanism of diphenylacetylene to diphenylethane hydrogenation on a PdAg surface (for more details, see Table S1).

It leads to a thermodynamic and kinetic favor of acetylene conversion into ethylene on the PdAg catalyst.

Further hydrogenation of the double bond on the Pd–Ag catalyst occurs through kinetic barriers of 28 and 26.5 kcal mol^{-1}, which are comparable with the hydrogenation barriers of DPA to DPE, respectively. Previously, it was shown that Pd catalyst modification with silver mainly changed the stability of adsorbed hydrocarbons rather than the activation energy.[27] The metal independence of the activation barriers for hydrogenation has also been observed in other hydrogenation reactions,[28] which indicates that the stability of the adsorbed species is the dominant parameter determining the potential activity and selectivity of the catalyst.

This study was supported by the Russian Science Foundation (grant no. 17-13-01526). We are grateful to Professor M. N. Vargaftik and Dr. I. A. Yakushev (N. S. Kurnakov Institute of General and Inorganic Chemistry, RAS) for supplying us with the initial $PdAg_2(OAc)_4(HOAc)_4$ complex. We are also grateful to the Department of Structural Studies of the N. D. Zelinsky Institute of Organic Chemistry, RAS for the materials characterization by electron microscopy and to Dr. G. I. Kapustin and N. A. Davshan for the catalyst study by CO chemisorption. M.G.M. acknowledges the computational resources (IBM Blue Gene/P supercomputer) provided by the Department of Computational Mathematics and Cybernetics of M. V. Lomonosov Moscow State University.

Online Supplementary Materials

Supplementary data associated with this article can be found in the online version at doi: 10.1016/j.mencom.2017.11.026.

References

1 V. P. Ananikov, K. I. Galkin, M. P. Egorov, A. M. Sakharov, S. G. Zlotin, E. A. Redina, V. I. Isaeva, L. M. Kustov, M. L. Gening and N. E. Nifantiev, *Mendeleev Commun*., 2016, **26**, 365.

2 V. P. Ananikov, D. B. Eremin, S. A. Yakukhnov, A. D. Dilman, V. V. Levin, M. P. Egorov, S. S. Karlov, L. M. Kustov, A. L. Tarasov, A. A. Greish, A. A. Shesterkina, A. M. Sakharov, Z. N. Nysenko, A. B. Sheremetev, A. Yu. Stakheev, I. S. Mashkovsky, A. Yu. Sukhorukov, S. L. Ioffe, A. O. Terent'ev, Vera A. Vil', Yu. V. Tomilov, R. A. Novikov, S. G. Zlotin, A. S. Kucherenko, N. E. Ustyuzhanina, V. B. Krylov, Yu. E. Tsvetkov, M. L. Gening and N. E. Nifantiev, *Mendeleev Commun*., 2017, **27**, 425.

3 X.-F. Yang, A. Wang, B. Qiao, J. Li, J. Liu and T. Zhang, *Acc. Chem. Res*., 2013, **46**, 1740.

4 J. Liu, *ACS Catal*., 2017, **7**, 34.

5 J. D. A. Pelletier and J.-M. Basset, *Acc. Chem. Res*., 2016, **49**, 664.

6 G. X. Pei, X. Y. Liu, A. Wang, A. F. Lee, M. A. Isaacs, L. Li, X. Pan, X. Yang, X. Wang, Z. Tai, K. Wilson and T. Zhang, *ACS Catal*., 2015, **5**, 3717.

7 G. X. Pei, X. Y. Liu, X. Yang, L. Zhang, A. Wang, L. Li, H. Wang, X. Wang and T. Zhang, *ACS Catal*., 2017, **7**, 1491.

8 P. V. Markov, G. O. Bragina, A. V. Rassolov, I. S. Mashkovsky, G. N. Baeva, O. P. Tkachenko, I. A. Yakushev, M. N. Vargaftik and A. Yu. Stakheev, *Mendeleev Commun*., 2016, **26**, 494.

9 P. V. Markov, G. O. Bragina, A. V. Rassolov, G. N. Baeva, I. S. Mashkovsky, V. Yu. Murzin, Ya. V. Zubavichus and A. Yu. Stakheev, *Mendeleev Commun*., 2016, **26**, 502.

10 G. Kyriakou, M. B. Boucher, A. D. Jewell, E. A. Lewis, T. J. Lawton, A. E. Baber, H. L. Tierney, M. Flytzani-Stephanopoulos and C. Sykes, *Science*, 2012, **335**, 1209.

11 A. V. Rassolov, P. V. Markov, G. O. Bragina, G. N. Baeva, D. S. Krivoruchenko, I. S. Mashkovskii, I. A. Yakushev, M. N. Vargaftik and A. Yu. Stakheev, *Kinet. Catal*., 2016, **57**, 859 (*Kinet. Katal*., 2016, **57**, 865).

12 A. V. Rassolov, P. V. Markov, G. O. Bragina, G. N. Baeva, I. S. Mashkovskii, I. A. Yakushev, M. N. Vargaftik and A. Yu. Stakheev, *Kinet. Catal*., 2016, **57**, 853 (*Kinet. Katal*., 2016, **57**, 857).

13 N. Yu. Kozitsyna, S. E. Nefedov, A. P. Klyagina, A. A. Markov, Zh. V. Dobrokhotova, Yu. A. Velikodny, D. I. Kochubey, T. S. Zyubina, A. E. Gekhman, M. N. Vargaftik and I. I. Moiseev, *Inorg. Chim. Acta*, 2011, **370**, 382.

14 P. V. Markov, G. O. Bragina, G. N. Baeva, O. P. Tkachenko, I. S. Mashkovskii, I. A. Yakushev, M. N. Vargaftik, and A. Yu. Stakheev, *Kinet. Catal*., 2016, **57**, 617 (*Kinet. Katal*., 2016, **57**, 621).

15 I. V. Yudanov, R. Sahnoun, K. M. Neyman, N. Rösch, J. Hoffmann, S. Schauermann, V. Johánek, H. Unterhalt, G. Rupprechter, J. Libuda and H.-J. Freund, *J. Phys. Chem. B*, 2003, **107**, 255.

16 H. L. Abbott, A. Aumer, Y. Lei, C. Asokan, R. J. Meyer, M. Sterrer, S. Shaikhutdinov and H.-J. Freund, *J. Phys. Chem. C*, 2010, **114**, 17099.

17 X. P. Xu and D. W. Goodman, *J. Phys. Chem*., 1993, **97**, 7711.

18 A. Yu. Stakheev, N. S. Smirnova, D. S. Krivoruchenko, G. N. Baeva, I. S. Mashkovsky, I. A. Yakushev and M. N. Vargaftik, *Mendeleev Commun*., 2017, **27**, 515.

19 C. Adamo and V. Barone, *J. Chem. Phys*., 1999, **110**, 6158.

20 S. Grimme, J. Antony, S. Ehrlich and H. Krieg, *J. Chem. Phys*., 2010, **132**, 154104.

21 C. C. Lovallo and M. Klobukowski, *J. Comput. Chem*., 2003, **24**, 1009.

22 C. C. Lovallo and M. Klobukowski, *J. Comput. Chem*., 2004, **25**, 1206.

23 W. J. Stevens, M. Krauss, H. Basch and P. G. Jasien, *Can. J. Chem*., 1992, **70**, 612.

24 N. Mardirossian and M. Head-Gordon, *Mol. Phys*., 2017, **115**, 2315.

25 M. G. Medvedev, I. S. Bushmarinov, J. Sun, J. P. Perdew and K. A. Lyssenko, *Science*, 2017, **355**, 49.

26 G. C. Bond, *Platinum Met. Rev*., 2000, **44**, 146

27 F. Studt, F. Abild-Pedersen, T. Bligaard, R. Z. Sørensen, C. H. Christensen and J. K. Nørskov, *Science*, 2008, **320**, 1320.

28 Z.-P. Liu and P. Hu, *J. Am. Chem. Soc*., 2003, **125**, 1958.

Received: 25th July 2017; Com. 17/5317